Self-consistent supercell approach to alloys with local environment effects

O. E. Peil,[1] A. V. Ruban,[2] and B. Johansson[2,3]
[1]*I. Institut für Theoretische Physik, Hamburg University, Hamburg, Germany*
[2]*Royal Institute of Technology, Department of Material Science & Engineering, SE-10044 Stockholm, Sweden*
[3]*Condensed Matter Theory Group, Department of Physics and Materials Science, Uppsala University, SE-75121 Uppsala, Sweden*
(Received 28 October 2011; revised manuscript received 10 March 2012; published 24 April 2012)

We present an efficient and accurate method for calculating electronic structure and related properties of random alloys with a proper treatment of local environment effects. The method is a generalization of the locally self-consistent Green's-function technique for the exact muffin-tin orbital method. An alloy system in the calculations is represented by a supercell with a certain set of atomic-distribution correlation functions. The Green's function for each atom in the supercell is obtained by embedding the cluster of neighboring atoms lying within a local interaction zone (LIZ) into an effective medium and solving the cluster Dyson equation exactly. The key ingredients of the method are locality, which makes it linearly scaling with the number of atoms in the supercell, and coherent-potential self-consistency of the effective medium, which results in a fast convergence of the electronic structure with respect to the LIZ size. To test the performance and accuracy of the method, we apply it to two systems: Fe-rich bcc-FeCr random alloy with and without a short-range order, and a Cr impurity on the Fe surface. Both cases demonstrate the importance of taking into account the local environment effects for correct description of magnetic and bulk properties.

DOI: 10.1103/PhysRevB.85.165140 PACS number(s): 71.23.−k, 71.20.Be, 75.50.Bb

I. INTRODUCTION

Accurate treatment of the electronic structure of disordered systems is a highly nontrivial problem, which requires the use of a proper statistical model. In the case of *metallic* random alloys on an ideal crystalline lattice, the simplest statistical averaging can be done for a single site leading to the translationally invariant effective medium best given by the so-called coherent-potential approximation (CPA).[1,2] The CPA constitutes the basis of most of the first-principles techniques for the electronic-structure calculations of random alloys, where it is usually combined with the multiple-scattering theory, or Korringa-Kohn-Rostocker (KKR),[3–5] and related methods.[6–8] Although the CPA has proven to be a quite successful approach for the electronic structure of many alloy systems, its application range is restricted either to completely random alloys and/or to alloys where local environment effects in the electronic structure are small, in the sense that their average is accurately given by the corresponding CPA effective medium.

The proper account of the local environment effects in the electronic-structure calculations, brought about either by correlated atomic distribution of alloy components (atomic short-range order) or by multisite electronic-structure correlations, can be done in several ways, which might be loosely subdivided into analytical Green's-function-based approaches, in which the nonlocality is taken into account by the summation of some subset of diagrams, and into supercell methods that make use of the self-averaging property of certain quantities, implying that the configurational averaging can be replaced with the averaging over a sufficiently large supercell.

The main objective of analytical approaches is to obtain a full Green's function or, alternatively, a self-energy of a disordered system. This is achieved by summing a large subset (ideally all) of diagrams corresponding to multiple scattering from different sites either for the whole system, like it is done in the augmented space formalism,[9] or for a specific set of clusters representing a given alloy system, as it is implemented in the cluster extensions of CPA.[10–12] The most developed example of this family of methods is the nonlocal CPA, which has been recently combined with first-principles calculations.[12–14] In this technique, the averaging is performed over all possible configurations of a specifically chosen cluster which tiles the entire underlying crystal lattice. In this case, as in similar analytical approaches, the average translational symmetry of the underlying lattice is lost together with the corresponding simple reciprocal space formalism, although it can be recovered with some additional effort.[14] However, to our knowledge, there has been no implementation of the nonlocal CPA within density functional theory (DFT) strictly consistent with the total charge density.

The requirement of the charge self-consistency is important not only for accurate total-energy calculations, but also because the correct account of the local environment effects themselves demands taking into consideration the response of the electronic density to the whole surrounding system, which can be fulfilled if the one-electron potential of every atom is determined in the DFT self-consistent way. The difficulty of achieving this self-consistency in Hamiltonian-based approaches, such as augmented space method, seems to be the main hurdle on the way to establish them as an accurate tool for the first-principles calculations of disordered alloys.

One of the ways to treat a disordered system within DFT self-consistently is to replace the configurational averaging by the averaging over a large sample, which is at the heart of supercell-based methods. These averagings are equivalent for an infinite-size sample and for quantities that possess the property of self-averaging, i.e. almost all observables of interest, including the Green's function and total energy. Moreover, if the interatomic interactions in the system are screened and hence short ranged, as it is the case for most metallic alloys, the size of the sample can be chosen to be reasonably small without introducing a significant error.[15]

In a naïve, or direct, implementation, one would set up a supercell with periodic boundary conditions, solve it exactly by, for instance, evaluating the Green's function of the entire supercell within a DFT code, and then average the onsite components of the Green's function for every component to get the alloy Green's function. This approach suffers from at least three serious problems: first, it can be computationally extremely demanding to find a Green's function of a large supercell since the complexity usually scales as the third power of the supercell volume; second, the Bloch states of a periodic system, with their infinite lifetimes, can not properly represent the states of a disordered alloy, and even after averaging over sites, the alloy Green's function would "feel" the periodicity, which may result, for example, in an ill-defined conductivity; and finally, the Brillouin zone (BZ) of the underlying lattice is shrunk to a small BZ of the supercell, and additional approximate routines are needed to restore the original translational symmetry. Note that the problem with Bloch states can be partially resolved by performing additional averaging over different realizations of the supercell, but this approach is obviously computationally expensive.

A method that overcomes all of the named problems is the locally self-consistent Green's-function (LSGF) technique.[16,17] The method, as it will be described below, combines the best features of both the analytical and supercell-based approaches and, in addition, it is manifestly charge self-consistent. In a historical perspective, it can be considered as a generalization and extension of the multishell, or embedded-cluster method (ECM),[18] and the locally self-consistent multiple-scattering (LSMS) method.[19]

The main idea of LSGF is that the local (onsite) Green's function for each atom in the supercell is determined from the Dyson equation restricted to the local interaction zone (LIZ) consisting of the given atom and its local environment embedded in the CPA-like effective medium, which is, in turn, built upon all the atoms residing on the alloy (sub)lattice. In this case, the periodic boundary conditions for the whole supercell are used only to determine the local environment of atoms close to the boundary of the supercell and for solving the Poisson equation in the electrostatic problem. The translational symmetry of the *underlying* lattice is used for solving the CPA equation for the effective medium and this method, thus, allows the use of the proper reciprocal-lattice formalism, avoiding at the same time the ideal nondecaying Bloch states in the case of alloys, which plague the direct supercell approach. Aside from the mentioned advantages, the computational complexity of LSGF scales linearly with the supercell size.

Certainly, the main playground of the LSGF method is the consistent and accurate calculations of the electronic structure of random alloys with or without short-range order. Also, increasing the size of the LIZ allows the systematic investigation of the local environment effects in alloy systems. Besides, it is a powerful tool for evaluating screened Coulomb interactions in random alloys.[20,21] At the same time, the application range of the method reaches far beyond homogeneous disordered systems. For example, by judiciously choosing the size of the LIZ to hide periodic images in a slab geometry, one can efficiently treat problems involving impurities on or near surfaces. In a similar way, the explicit evaluation of the interatomic interactions between a pair or multiple of impurities in the host metal is possible. The Green's-function approach embodied in the method provides additional benefits in treating paramagnetic random systems. Some examples of such applications will be presented in this paper.

The previous practical realization of the LSGF method was done using the KKR method within atomic sphere approximation (ASA).[17,22] The KKR-ASA method itself suffers from the normalization error: electronic states are normalized within Wigner-Seitz spheres instead of Wigner-Seitz cells. This leads, in turn, to a quite substantial error in the total energy, making, for instance, practically impossible the accurate calculations of the total-energy variations related to the deformation of the crystal structure. At the same time, the LSGF approach is a general formalism that can be implemented in any code based on multiple-scattering theory. In this paper, we describe the implementation within the exact-muffin-tin-orbital (EMTO) method.[23–26] The method belongs to the family of screened KKR techniques with the basis set formed by so-called third-generation muffin-tin (MT) orbitals introduced by Andersen.[23] During the last decade, this method, combined with the full-charged-density technique, has proven to be sufficiently accurate in calculations of a wide spectrum of alloy properties.[26]

The paper consists of two main parts. In the first part, namely, Sec. II, we describe the LSGF formalism, starting with some details of the EMTO method that are essential for understanding the implementation. In the second part, Sec. III, we provide the results of test calculations followed by real calculations demonstrating the ability of the method to treat both homogeneous random alloys, magnetic, as well as nonmagnetic, and inhomogeneous systems, such as surfaces. In the last section, we conclude the results and briefly discuss possible extensions of the current LSGF implementation.

II. METHOD

As has been mentioned in the Introduction, in LSGF, one starts from building a supercell with periodic boundary conditions by replicating a unit cell of the underlying lattice. The supercell is populated with components in any desired (random or ordered) configuration (see Sec. II B). The main ingredients of the EMTO-LSGF (ELSGF) approach are the supercell setup, EMTO method itself, and LSGF part involving the solution of the restricted Dyson equation.

The EMTO part (more generally, the KKR part) of the ELSGF method runs similar to the usual EMTO-CPA implementation, as far as it concerns the effective medium, density of states, charge density, and total energy. The full symmetry of the underlying lattice is employed, reflecting the single-site character of the effective medium. After the effective medium is found, the cluster path operator is evaluated using the ECM, or restricted Dyson equation, for each atom in the supercell. This cluster path operator is subsequently used for the normalization of states, determining the density of states, charge density, and total energy.

In this section, we first briefly outline the EMTO Green's-function formalism and the features specific to its implementation within the LSGF technique. Then, we present strategies for choosing a proper supercell, and finally describe the LSGF formalism within EMTO. Details concerning the structure

constants, the construction of the optimized one-electron potential, the full charge density, as well as the total-energy calculations within the full-charge-density formalism, are the same as in the usual EMTO method, and their comprehensive description can be found in Refs. 25 and 26.

A. EMTO Green's-function formalism

The main idea behind the EMTO method is to keep the simplicity of the MT or screened KKR method by making use of the muffin-tin geometry of the one-electron potential, but to improve the accuracy of the electronic-structure calculations to the level of the full potential methods. The latter can be achieved by replacing usual MT spheres with large overlapping MT spheres, which allow a better approximation for the full potential. At the same time, additional nonoverlapping screening spheres are used to define boundary conditions for the solutions (referred to as screened spherical waves) in the interstitial region.

The path operator $g(z)$ is defined as follows:

$$\sum_{\mathbf{R}''L''} K^a_{\mathbf{R}'L'\mathbf{R}''L''}(z) g_{\mathbf{R}''L''\mathbf{R}L}(z) = \delta_{\mathbf{R}\mathbf{R}'}\delta_{LL'}, \tag{1}$$

with the kink operator

$$K^a_{\mathbf{R}'L'\mathbf{R}L}(z) = a_{\mathbf{R}'} S^a_{\mathbf{R}'L'\mathbf{R}L}(\kappa^2) - \delta_{\mathbf{R}\mathbf{R}'}\delta_{LL'} a_{\mathbf{R}} D^a_{\mathbf{R}l}(z), \tag{2}$$

where $a_{\mathbf{R}}$ is the screening-sphere radius at site $\mathbf{R}$, $S^a_{\mathbf{R}'L'\mathbf{R}L}(\kappa^2)$ the screened structure constants depending on energy $\kappa^2 = z - \upsilon_0$ defined with respect to the muffin-tin zero υ_0, and $D^a_{\mathbf{R}l}(z)$ the potential function determined as usual by the logarithmic derivative of the partial waves at the MT sphere. Note the sign convention for the potential function and structure constants.

For systems with translational symmetry, the onsite path operator is determined as

$$g_0(z) = \frac{1}{\Omega_{\mathrm{BZ}}} \int_{\mathrm{BZ}} \frac{d\mathbf{k}}{S(\mathbf{k},z) - D(z)}, \tag{3}$$

where integration is performed over the Brillouin zone of the crystal lattice. We write all expressions for a one-atom Bravais lattice for clarity; the extension to multiple-atom basis is straightforward.

To evaluate the density of states (DOS), the path operator must be properly normalized with the overlap matrix. The overlap matrix in the EMTO formalism is given by $\dot{K}^a_{\mathbf{R}'L'\mathbf{R}L}(z)$, the energy derivative of the kink operator. The number of states is then

$$\mathcal{N}(\varepsilon) = -\frac{1}{\pi} \int_{C_\varepsilon} dz\, [G(z) - D_{\mathrm{poles}}(z)], \tag{4}$$

$$G(z) = \frac{1}{\Omega_{\mathrm{BZ}}} \int_{\mathrm{BZ}} d\mathbf{k}\, \frac{\dot{S}(\mathbf{k},z) - \dot{D}(z)}{S(\mathbf{k},z) - D(z)}, \tag{5}$$

where the integration along the half of the contour embracing the valence band below energy ε is performed, and pole contributions D_{poles} coming from the poles of $1/D(z)$ and $\dot{D}(z)$, are subtracted. The Fermi energy ε_F is found from the condition $\mathcal{N}(\varepsilon_F) = N_{el}$, where N_{el} is the number of the valence electrons.

In the case of a random alloy on a lattice, the CPA equations are used to determine the electronic structure given by the coherent path operator $\tilde{g}$ through the corresponding coherent potential operator $\tilde{D}$ of the single-site effective medium:

$$\tilde{g}(z) = \frac{1}{\Omega_{\mathrm{BZ}}} \int_{\mathrm{BZ}} \frac{d\mathbf{k}}{S(\mathbf{k},z) - \tilde{D}(z)}. \tag{6}$$

The path operators of the ith alloy component g_i are found via the single-site Dyson equation

$$g_i = \tilde{g} + \tilde{g}(\tilde{D} - D_i) g_i, \tag{7}$$

from which the coherent path operator is determined as

$$\sum_i c_i g_i = \tilde{g}, \tag{8}$$

where c_i is the concentration of alloy components. The last three CPA nonlinear equations are solved self-consistently.

In EMTO CPA, the correctly normalized Green's function and number of states (per Wigner-Seitz cell) are determined as

$$\mathcal{N}(\varepsilon) = -\frac{1}{\pi} \int_{C_\varepsilon} dz\, [G(z) - D_{\mathrm{poles}}(z)], \tag{9}$$

$$G(z) = \frac{1}{\Omega_{\mathrm{BZ}}} \int_{\mathrm{BZ}} d\mathbf{k}\, \frac{\dot{S}(\mathbf{k},z) - \sum_i c_i \dot{D}_i(z)}{S(\mathbf{k},z) - \tilde{D}(z)}, \tag{10}$$

and the pole contributions are weighted by concentrations c_i accordingly.

B. Supercell

In the LSGF calculations, an alloy system is represented by a supercell model. In general, creating a supercell with needed statistical properties, given by its atomic-distribution correlation functions, is a highly nontrivial task, mathematically equivalent to the optimization of a many-variable function in a multidimensional space. The initial building block of the supercell is determined by the underlying lattice containing N_q basis atoms. Let us note that the choice of the initial unit cell of the supercell is quite arbitrary, and such a unit cell can be different from that of the underlying crystal lattice in the subsequent LSGF calculations, provided that the supercell is conformal to the underlying lattice. A simple example is the choice of the cubic unit cell containing two atoms in the case of bcc structure as a building block of the supercell and the use of the bcc translational symmetry in the LSGF calculations. In general, the choice of the unit cell is motivated by the model of an alloy system that may have several different sublattices with different compositions and distributions of alloying elements [for an application of ELSGF to a rather complex example of the FeCr σ-phase with 30 atoms per unit cell subdivided into 5 nonequivalent sublattices with distinct compositions (see Ref. 27)].

The setup of the supercell starts from the definition of a desired alloy configuration by characterizing its atomic correlation functions that can be defined in different ways. For a homogeneous binary alloy, for instance, they can be given by the average products of spinlike variables σ_i, taking on values $+1$ or -1, depending on which alloy component

occupies site i:

$$\xi_f^{(n)} = \langle \sigma_i \sigma_j \dots \sigma_k \rangle_f, \tag{11}$$

where $\xi_f^{(n)}$ is the n-site correlation function for cluster f, and $\langle \dots \rangle$ is the average over the supercell. A completely disordered configuration is given by $\xi_f^{(n)} = \sigma^n$, with $\sigma = 2c - 1 \equiv \xi^{(1)}$, where c is the concentration of one of the alloy components.

Although this definition is easily generalized to the case of multicomponent and inhomogeneous random alloys, where different sublattices with different alloy compositions and atomic short-range order are present, it is extremely difficult to use it in practice. The main obstacle here is the finite and quite restricted size of the supercell. For instance, the number of sites in the supercell, N, defines the possible concentrations to be only k/N, where $k = 0, 1, \dots, N$. Much more severe restrictions to the possible pair and multicorrelation functions originate from the geometry of the underlying lattice, e.g., from the number of possible clusters (coordination number for pair-correlation functions). Nevertheless, a supercell consisting of about 500–2000 sites is usually sufficiently big to model a large variety of alloy systems, especially taking into consideration our restricted knowledge about atomic-distribution correlation functions in real alloys.

The main condition for a supercell to be a valid representation of a random alloy with a specific short-range order is to have the same correlation functions as the given alloy for those clusters f (or coordination shells in case of pair-correlation functions) which affect a physical property of interest. If the cluster expansion is applicable to a particular observable A, then the *relevant* clusters are those for which expansion coefficients A_f have nonzero (in practice non-negligible) values:

$$A = \sum_f A_f \xi_f. \tag{12}$$

Here, we do not discuss for which physical properties such an expansion can be valid in general, and how fast the expansion converges, but as an example we can mention the total energy of an alloy which, as usually tacitly assumed, can be expanded in this way. The coefficients A_f are then just the effective interactions of the corresponding Ising Hamiltonian.

Let us note that a finite supercell of a restricted size can not represent a random alloy in general (and called "random" for that matter): the same supercell can be "random" for the same system for one property and "ordered" for the other, not mentioning different systems. In principle, one should check the configurational dependence of the observable of interest (or ideally to find out coefficients A_f) prior to using a supercell as a random-alloy model. For instance, the expansion coefficients of the total energy are related to the effective interatomic interactions that can be found either with the aid of the generalized perturbation method within single-site CPA or with the cluster inversion method.

In LSGF, the *real* correlations of the supercell are only taken into consideration inside the LIZ, while outside the LIZ, the correlation functions correspond to a completely random alloy. An observable calculated by the LSGF method is given by the following formula:

$$A^{\mathrm{LSGF}} = \sum_{f \in \mathrm{LIZ}} A_f \xi_f + \sum_{f \notin \mathrm{LIZ}} A_f \xi_f^{\mathrm{rand}}, \tag{13}$$

where $\xi_f^{\mathrm{rand}} \equiv \xi_f^{(n)-\mathrm{rand}} = \sigma^n$ are the correlation functions of the completely random alloy. The condition for the cluster to belong to the LIZ is that one of its vertices coincides with the position of the central atom, and all cluster atoms belong to the LIZ. This condition will be elaborated in the next sections, where we give the details of the electronic-structure calculations with the LSGF method.

The electrostatic energy is calculated "exactly" for a given supercell. This means that the summation is not restricted to the LIZ, but is rather performed over the entire periodic infinite system. In principle, this may result in a spurious electrostatic interaction between periodic images. Fortunately, in most metallic alloys, the pair interactions are screened, the screening length being rather small. The important condition that the range of the pair-correlation function and the screening length are within a supercell can, thus, be easily satisfied for supercells containing several hundred atoms.

C. ELSGF

Given a supercell containing N atoms, the calculation of the electronic structure within the ELSGF method starts from the determination of the translationally invariant CPA effective medium built upon all the atoms on a corresponding (sub)lattice. In the simplest case of a Bravais lattice, corresponding CPA equations are similar to Eqs. (6)–(8):

$$\bar{g}_0 = \frac{1}{\Omega_{\mathrm{BZ}}} \int_{\mathrm{BZ}} d\mathbf{k} \frac{1}{S(\mathbf{k}, z) - \bar{D}(z)}, \tag{14}$$

$$g_i = \bar{g}_0 + \bar{g}_0 (\bar{D}_0 - D_i) g_i, \tag{15}$$

$$\bar{g}_0 = \frac{1}{N} \sum_i g_i, \tag{16}$$

Here, $\bar{g}_0$ and $\bar{D}$ are the onsite effective-medium path operator and logarithmic derivative; g_i is the onsite path operator of site i. These nonlinear equations are solved self-consistently for $\bar{D}$ and $\bar{g}$ for a given set of one-electron potentials in the supercell. Equations (14)–(16) are the CPA equations for an N-component alloy. This makes the effective-medium single site self-consistent and all translational and point symmetries of the underlying lattice are preserved. In addition, a connection to the CPA guarantees the analyticity of the effective medium and hence of its real-space path operator determined as

$$\bar{g}_{ij} = \frac{1}{\Omega_{\mathrm{BZ}}} \int_{\mathrm{BZ}} d\mathbf{k} \frac{e^{i\mathbf{k}(\mathbf{R}_i - \mathbf{R}_j)}}{S(\mathbf{k}, z) - \bar{D}(z)}, \tag{17}$$

where $\mathbf{R}_i$, $\mathbf{R}_j$ are the positions of sites i and j of the lattice.

Once the effective medium is defined, the electronic structure for every site can be determined by solving the multiple-scattering problem for the LIZ cluster embedded into the effective medium, which enables one to take the local environment effects into consideration. The size of the LIZ is usually defined as a number of coordination shells constituting the cluster centered around a given atom, with the LIZ of size one (LIZ = 1) corresponding to the cluster consisting of a

single central atom. The rest of the system outside the LIZ is given by the effective medium.

The multiple-scattering problem for such a setup is solved *exactly* with the aid of the Dyson equation as it is done in the embedded cluster method (ECM).[18] Consider a LIZ cluster given by atoms with potential functions D_i, where i runs over cluster sites $\mathbf{R}_i$. The cluster is embedded into the effective medium defined by a real-space path operator $\bar{g}_{ij}$ and a coherent potential function $\bar{D}_i$. The path operator of the cluster g_{ij} is then found within the ECM as

$$g_{ij} = \bar{g}_{ij} + \sum_k \bar{g}_{ik}(\bar{D}_k - D_j)g_{kj}, \tag{18}$$

from which one finds immediately

$$g_{ij} = \sum_k \left[1 - \sum_{k'} \bar{g}_{ik'}(\bar{D}_{k'} - D_k)\right]^{-1} \bar{g}_{kj}. \tag{19}$$

The Fermi energy of the system, ε_F, is determined from the normalization condition $\mathcal{N}(\varepsilon_F) = N_{el}$ for the number of electron states in the supercell N_{el}, where the number of states is defined in a way similar to that in the EMTO method:

$$\mathcal{N}(\varepsilon) = -\frac{1}{\pi}\int_{C_\varepsilon} dz\, [G(z) - D_{\text{poles}}(z)], \tag{20}$$

with the Green's function $G(z)$ having an additional contribution compared to that of the EMTO-CPA Green's function Eq. (10). The point is that unlike the EMTO CPA, where the states are normalized within a single-site Wigner-Seitz cell, the states in ELSGF are normalized within the entire LIZ. Starting from the expression for the Green's function in EMTO CPA (10), rewriting it in the real space, and replacing the effective-medium path operator by the cluster path operator within the LIZ, one gets

$$G(z) = \frac{1}{N}\sum_i \left[\frac{1}{\Omega_{\text{BZ}}}\int_{\text{BZ}} d\mathbf{k}\, \frac{\dot{S}(\mathbf{k},z) - \dot{D}_i(z)}{S(\mathbf{k},z) - \bar{D}(z)} + \sum_j (g_{ij} - \bar{g}_{ij})\dot{S}_{ji}\right]. \tag{21}$$

The electron density for each site is obtained from the onsite path operator $g_i \equiv g_{ii}$ in the same way as it is done in the EMTO method.[26] The DFT self-consistency loop is then closed by evaluating the one-electron potential for every site, assuming the translational symmetry (periodic boundary conditions) for the entire supercell in order to solve the electrostatic problem exactly for each site. Finally, after the self-consistency is reached, the full charge density is determined in order to perform accurate calculations of the total energy of the supercell.[25,26]

D. Disordered-local-moment model for the LIZ

Accurate calculations of the electronic structure and energetics of paramagnetic alloys with the finite magnitudes of local magnetic moments on atoms present a challenge for modern first-principles methods. As has been proven in Ref. 28, if the magnitude of the local magnetic moments does not fluctuate strongly and the spin-orbit coupling is negligible, such a state is accurately described by the collinear disordered-local-moment (DLM) model, where atoms with spin-up and spin-down orientations of their local magnetic moment are distributed randomly on the underlying lattice.

Although the DLM configuration can be modeled by a supercell with randomly distributed atoms having different spin orientations, such a naïve supercell representation can, in fact, lead to incorrect results because in reality, magnetic degrees of freedom fluctuate (transverse fluctuations are implied here) rapidly and create, thus, a local environment different from the one with static magnetic moments. In this sense, a CPA-based scheme seems to be a better method to calculate the systems in the DLM state. Besides, a supercell model with randomly distributed static moments becomes too cumbersome since specific atomic correlations should be set up not only between alloy components, but also between their spin-up and -down counterparts.

Within the LSGF method, a straightforward DLM-CPA implementation is possible only in the single-site mode (LIZ = 1), when the required CPA averaging and thus the Dyson equation for every site and spin can be solved for the appropriately spin-averaged effective medium. However, this simple scheme obviously breaks down when the nearest-neighbor atoms are included in the LIZ. The problem here is that the potential functions of the neighbors of the central atom would incorrectly correspond to a specific magnetic configuration rather than the random one, as it should be in the DLM state.

Clearly, a correct description of the DLM state implies here that the central atom "sees" its neighbors inside the LIZ in spin-averaged states. Such a solution can be efficiently implemented in the LSGF method by performing partial constrained averaging of the spin states for all the sites inside the LIZ except the central one. This amounts to choosing an appropriate effective potential of a given atom in the same way as it is usually done within CPA DLM. To be more specific, we start by defining the onsite path operators in two spin channels by solving corresponding single-site Dyson equations

$$g_i^{\uparrow} = [1 - \bar{g}_0(\bar{D} - D_i^{\uparrow})]^{-1}\bar{g}_0, \tag{22}$$

$$g_i^{\downarrow} = [1 - \bar{g}_0(\bar{D} - D_i^{\downarrow})]^{-1}\bar{g}_0. \tag{23}$$

A partially averaged (DLM-averaged) path operator is then introduced for each site and global spin channel σ as

$$\langle g_i\rangle_\sigma = \tfrac{1}{2}(g_i^{\uparrow} + g_i^{\downarrow}). \tag{24}$$

The paramagnetic effective medium is now determined from these DLM-averaged path operators, with the self-consistency condition being

$$\bar{g}_0 = \frac{1}{N}\sum_i \langle g_i\rangle_\sigma. \tag{25}$$

Once the effective medium is determined, one can use the equation

$$\langle g_i\rangle_\sigma = \bar{g}_0 + \bar{g}_0(\bar{D} - \langle D_i\rangle_\sigma)\langle g_i\rangle_\sigma \tag{26}$$

to find a corresponding DLM-averaged potential function for each site:

$$\langle D_i \rangle_\sigma = \bar{D} - \bar{g}_0^{-1} + \langle g_i \rangle_\sigma^{-1} . \quad (27)$$

We then solve Eq. (18) for each site assuming that all the atoms in the LIZ surrounding the central one are in the paramagnetic state. The potential function for each noncentral atom in the cluster is thus replaced by a DLM-averaged potential function. Specifically, for a given cluster with a central site i, the cluster potential function D_j is defined as follows:

$$D_j^\sigma = \begin{cases} D_i^\sigma , & j = i \\ \langle D_j \rangle_\sigma , & \text{otherwise.} \end{cases} \quad (28)$$

III. TESTS AND RESULTS

A basic test for the ELSGF method is the convergence of quantities of interest (the total energy in the first place) with respect to the size of the LIZ. By construction, the method observes two limits: LIZ $\to \infty$ ($N \to \infty$), corresponding to the formally exact solution of the Dyson equation for the entire system; LIZ = 1, equivalent to the CPA with the correct account of electrostatics (sometimes referred to as the isomorphous CPA). In-between these two limiting cases, the convergence with respect to the LIZ depends pretty much on the observable or, more strictly, on how fast the cluster expansion coefficients decay with distance, as has already been emphasized in Sec. II B. In particular, the expansion coefficients of the total energy are related to effective interactions, and the convergence test can be used as a rough estimate of the range of the effective interactions.[17] An example of such a calculation is given below.

Later in this section, we demonstrate some of the capabilities of the ELSGF method by applying it to real systems. Emphasis is made on the effects of short-range order, especially in magnetic systems. Also, a surface-segregation problem is considered as an example of an inhomogeneous system.

A. Range of the relevant correlation functions from ELSGF

The direct relation between the convergence with the LIZ size and the range of the correlation functions makes it possible to estimate the latter by varying the size of the LIZ in LSGF calculations. As has been discussed in Sec. II B, if an observable is self-averaging and can be expanded in terms of the atomic-distribution correlation functions, the expansion is given by Eq. (13) within LSGF. According to this equation, the correlation functions beyond the LIZ correspond to those of a completely disordered alloy, and thus, by calculating a completely ordered alloy with LSGF, one captures only contributions from the correlation functions corresponding to the LIZ cluster. In view of this, one can estimate the range of the relevant correlations as the minimal size of the LIZ that provides the same result as the one given by a direct *ab initio* calculation for the given ordered structure.

As an example, we present here results for the DOS and the total energy of a completely ordered B2-NiAl phase, also

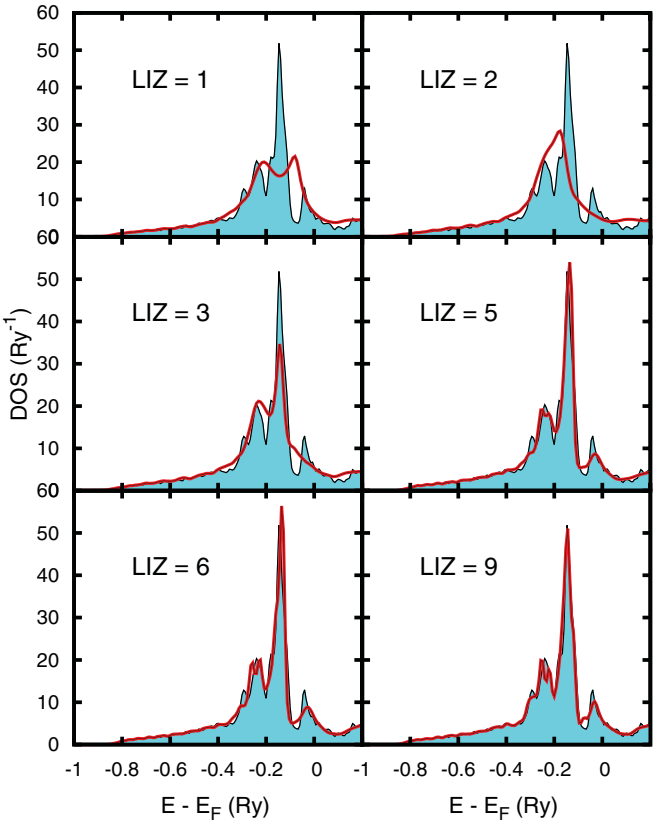

FIG. 1. (Color online) The DOS for B2-NiAl obtained in the ELSGF calculations with different LIZ sizes (thick red) compared to a direct calculation (shaded region). LIZ = 1 corresponds to a single-site approximation, but different from CPA, because the electrostatic potential is calculated for the ordered structure.

considered in Ref. 17. Let us note that this ordered phase represents the worst possible case for the LSGF method since its every coordination shell consists of atoms of only one type, while in a random alloy with the same equiatomic composition, the number of atoms of both types should be equal (on average). Formally, this is given by the corresponding atomic-correlation functions, or Warren-Cowley short-range-order (SRO) parameters, which take on values $\alpha_i = -1,1,1, -1,1,1, -1, \ldots$ for the first several coordination shells in the B2 structure. Here, -1 (1) corresponds to the case when every atom has only atoms of the opposite (same) type at the corresponding coordination shell, while the SRO parameters are zero in the case of a random alloy without short-range-order effects.

In Fig. 1, we show the DOS of the B2-NiAl phase obtained in the ELSGF calculations with different sizes of the LIZ, together with the DOS calculated by the EMTO method. One can see that at least four coordination shells (LIZ = 5) need to be included in the LIZ to reproduce the main features of the DOS with a reasonable accuracy, and still some small DOS features are not well reproduced even when eight coordination shells (LIZ = 9) are included.

A similar but a bit more interesting example is shown in Fig. 2 where the ELSGF calculations of the DOS of B2-FeSi presented. This system has unusual magnetic properties very sensitive to the local environment. In particular, there is quite

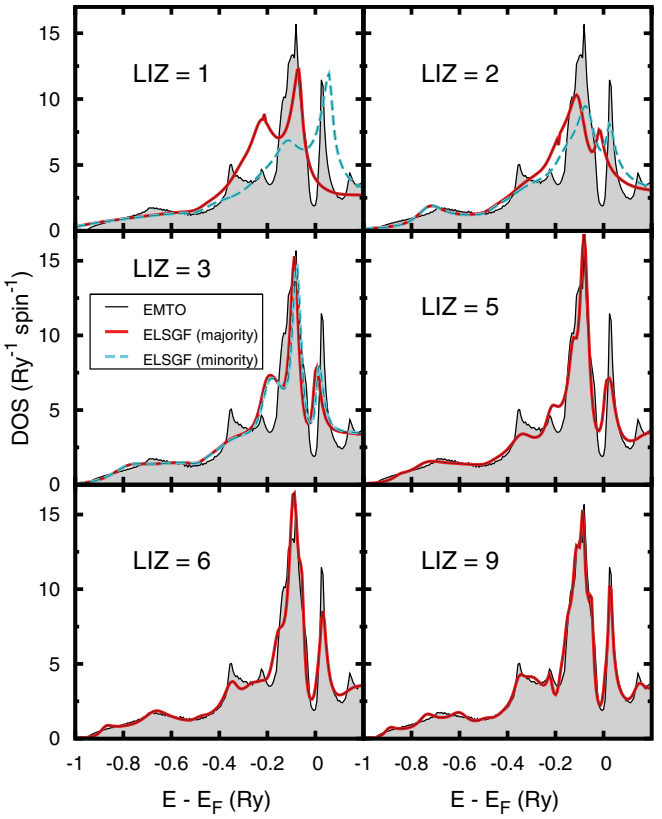

FIG. 2. (Color online) The DOS for B2-FeSi obtained in the ELSGF calculations with different LIZ sizes (thick solid-red and dashed-cyan lines) compared to a direct calculation (shaded region). LIZ = 1 corresponds to a single-site approximation, but different from CPA, because electrostatic potential is calculated for the ordered structure.

large magnetic moment in bcc random $Fe_{0.5}Si_{0.5}$ alloy, but it disappears in the B2 ordered structure. By performing the ELSGF calculations of the B2 structure with increasing LIZ, one can find the effect of every coordination shell on the magnetic moment. As one can see in Fig. 2, there is an obvious splitting of the bands in the single-site approximation (LIZ = 1, equivalent to the isomorphous CPA, but with incorrect electrostatic potential, which is determined for the B2 structure).

The inclusion of the first coordination shell in the LIZ (LIZ = 2) results in a substantial reduction of the splitting. In this case, Fe atoms can see nearest-neighbor Al atoms (and vice versa, Al atoms are surrounded be Fe atoms at the first coordination shell), while the rest of the crystal is represented by the CPA effective medium. Thus, such a large reduction of the magnetic moment of Fe seems to be obvious in this case. The next, second, coordination shell of Fe atoms in the B2 structure consists of only Fe atoms, and thus one could expect a slight increase of the magnetic moment due to additional Fe-Fe interactions when the LIZ size increases from two to three. However, the splitting and magnetic moment are further reduced, and when the next, third coordination shell is included in calculations, the magnetic moment becomes practically zero (see Fig. 3). This indicates that most probably the Fe-Fe

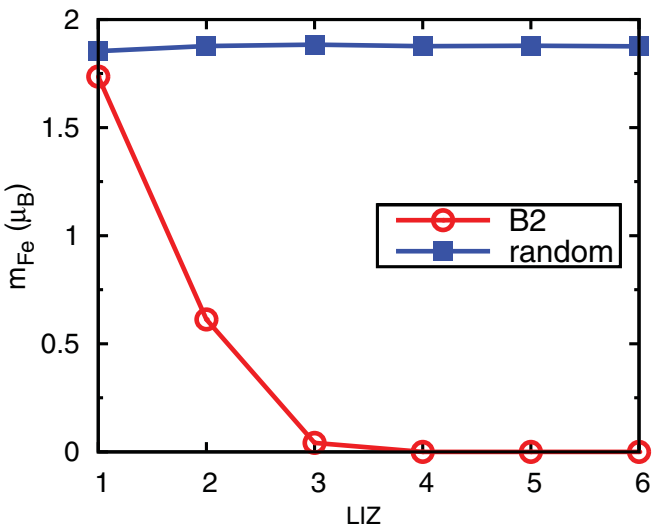

FIG. 3. (Color online) Local (average over the random alloy) magnetic moment of Fe in the ELSGF calculations of B2 structure and an equiatomic random alloy as a function of the LIZ size.

exchange interaction parameters are antiferromagnetic in this case.

For comparison, we also show in Fig. 4 the DOS of random $Fe_{0.5}Si_{0.5}$ alloy calculated by the ELSGF. In this case, the supercell consisting of 256 atoms [$4 \times 4 \times 8(\times 2)$] atoms has been used, the atomic-distribution pair-correlation functions of which were as in the random alloy up to the eighth coordination shell. The DOS for LIZ = 1 (isomorphous CPA model) is actually very close to that for the B2 phase shown in Fig. 2. The inclusion of the first coordination shell in the LIZ leads to a slight modification of mostly the spin-majority band, while the inclusion of more distant coordination shells to a slight change of the minority spin band. In Fig. 4, we show only the result for LIZ = 6 (five coordination shells included in the calculations). However, this result is practically indistinguishable from those for the LIZ = 4 and 5.

The relatively fast convergence of the DOS with the LIZ size for random alloys is a natural feature of the LSGF calculations with the CPA effective medium. The better the CPA works, the faster convergence. In most cases, the inclusion just of the first coordination shell in the LIZ provides very accurate description of the DOS of random alloys. In the case of Fe-Si, it is a bit slow, exhibiting distant "local environment effect," which is most probably connected with the nontrivial magnetism in this system, also showing up in the ELSGF calculations of the B2-FiSi.

The evolution of the density of states with increasing LIZ gives an idea of how fast the electronic structure approaches the one for an ordered system with the inclusion of the corresponding interactions, thereby providing an estimate of the range of the correlation functions responsible for specific features of the DOS. An important and interesting point here, however, is that although the DOS is directly related to the total energy (specifically, to the band energy), its details are not important for the energy value, and the convergence of the total energy with respect to the LIZ size can thus be much faster. This is partly due to the integral dependence of the total energy on the DOS. This point is illustrated in Figs. 5 and 6,

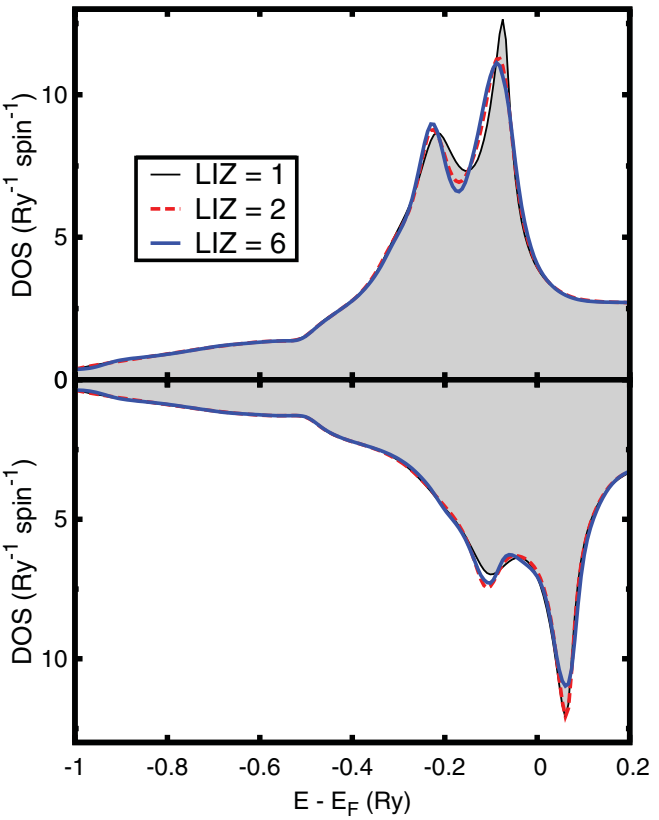

FIG. 4. (Color online) The DOS of the random bcc $Fe_{0.5}Si_{0.5}$ alloy obtained in the ELSGF calculations with different LIZ sizes: LIZ = 1 corresponds to the single-site CPA (shaded area), LIZ = 2 (thick dashed red line) and 6 (thick solid blue line) are the results with local environment effects up to the first and fifth bcc coordination shells, respectively. The spin-majority band is shown in the upper panel and the spin-minority band in the bottom panel.

where we show the convergence of the total energy of B2 NiAl and FeSi, respectively, as a function of the LIZ size.

One can clearly see that in the case of the B2-NiAl, already starting from the LIZ corresponding to the first coordination shell (LIZ = 2), the difference in the total energy becomes very small and remains so for larger LIZ. As was shown in Ref. 17, the change of the total energy with the LIZ size can be traced back to the strength of the effective intersite interactions entering the Ising configurational Hamiltonian. For this particular case of NiAl binary alloy, it can be written as

$$H = \frac{1}{2}\sum_{p}\sum_{i,j\in p} V_p^{(2)}\delta c_i \delta c_j + \ldots, \qquad (29)$$

where summation runs over coordination shells p and the corresponding sites of the lattice i and j; $V_p^{(2)}$ are effective pair interactions and $\delta c_i = c_i - c$ the concentration fluctuation of the occupation number c_i, which takes on values 1 and 0, depending on which alloy component occupies site i.

For the system considered, one can, in fact, estimate the value of effective interactions. Figure 5 shows that the strongest interaction is the one related to the first coordination shell. Assuming that it is the pair effective interaction that is dominant at the first coordination shell, its value could be

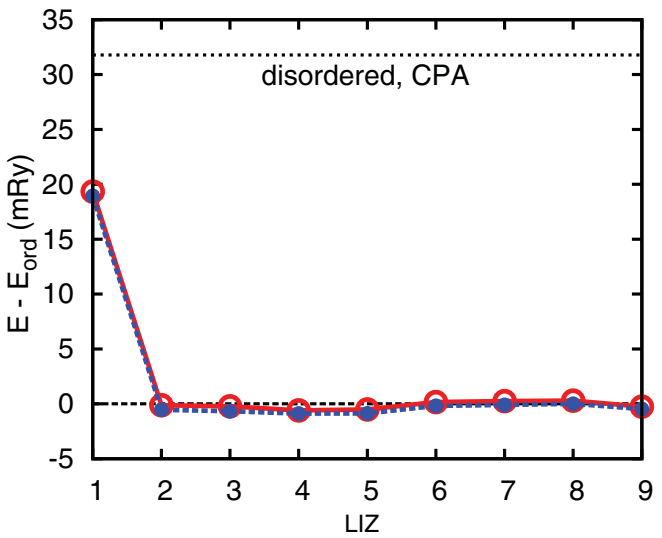

FIG. 5. (Color online) Convergence of the total energy with respect to the size of the LIZ for B2-NiAl. The difference between ELSGF (EMTO CPA: dotted line) and EMTO total energies are shown. Red solid line (open circles): MT basis with $l_{max} = 3$; blue dashed line (filled circles): MT basis with $l_{max} = 2$.

assessed as just the difference between the total energy of a random alloy and that of the ordered one with LIZ = 2 (which includes the first coordination shell), i.e., $V_1^{(2)} \sim 32$ mRy [factor 1/8 in Eq. (29) is canceled exactly by the bcc coordination number 8]. However, one should be aware of the fact that such a simple estimation is valid only in the case when the contribution from multisite interactions is small compared with that from the pair interactions. At the same time, there are quite a few multisite interactions contributing even in the case of LIZ = 2, when only the first coordination shell is included in the calculations since they are for all the possible clusters in the LIZ with one site being the central site of the LIZ.

One can also see in Fig. 5 that the total energy of the B2-NiAl for LIZ = 1, which is the single-site approximation,

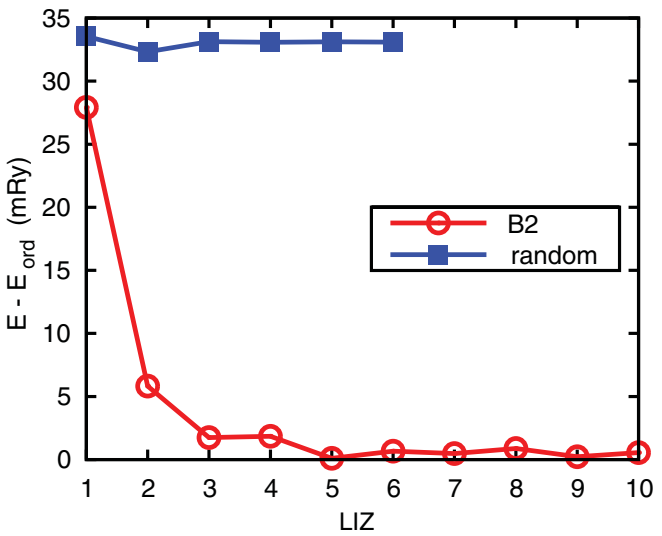

FIG. 6. (Color online) Convergence of the total energy with respect to the size of the LIZ for the B2 and random FeSi alloys.

is not equal to that of the random alloy obtained from the CPA, although LSGF with LIZ = 1 is formally equivalent to the CPA. The reason for the difference is the electrostatic energy, which is calculated in LSGF for the entire supercell representing an ordered system in our case. The difference between the LSGF result with LIZ = 1 and the energy of the random alloy can be roughly associated with the electrostatic part of the effective interactions, or a so-called intersite screened Coulomb interaction.[29]

In Fig. 6, we show the results of similar calculations but for the ordered B2 and random FeSi alloys. One can see that the convergence of the total energy of the B2 phase with respect to the LIZ size is worse than in the case of B2-NiAl. Another reason for that, apart from the convergence of the effective interactions, can be the fact that the FM state is stable up to LIZ = 3. The existence of quite long-range local environment effects in the random FeSi alloy has been already discussed above for the DOS. It also leads to the unusually slow convergence of the total energy of random alloy, which is as a rule quite accurate already for the LIZ = 2, when the first coordination shell is included in the LIZ.

B. Short-range-order effects in random FeCr alloys

One of the advantages of the LSGF method is the fact that the computational complexity scales linearly with the number of atoms, which renders possible accurate first-principles calculations for systems containing up to several thousand atoms. Such a size of a supercell allows one to model a large variety of alloys with various concentrations and atomic short-range orders. In this section, we demonstrate such a possibility for the case of ferromagnetic Fe-rich Fe-Cr alloys, which have attracted great attention of scientists in different fields owing to potential applications of these alloys in industry.

From a scientific point of view, this system is quite interesting and complicated when it comes to its accurate first-principles description. One of the reasons is a complex interplay of magnetism at zero as well as at elevated temperatures and interatomic interactions and, consequently, thermodynamic properties of these alloys.[30–34] In particular, the type of alloying abruptly changes with Cr concentration and temperature[33,35,36] in the composition range of up to about 20 at.% Cr. While there is a quite strong ordering tendency between Fe and Cr atoms at low temperatures in the ferromagnetic state and at low Cr concentration, Fe-Cr alloys exhibit a phase-separation behavior at higher temperatures, close to and above the Curie temperature, and with increasing Cr content. It was also demonstrated in Ref. 34 that the usual Ising model breaks down for this system due to a strong local environment dependence of the effective interactions.

It is clear that real Fe-Cr alloys must have a certain amount of atomic short-range order, and its type and magnitude depend on the thermal treatment of alloy samples. At the same time, practically all calculations for random Fe-Cr alloys are done for completely random-alloy configurations (in fact, with rare exceptions, these are just CPA-based calculations). In this section, we investigate the effect of the atomic short-range order on some of the ground-state and elastic properties of the Fe-rich FeCr alloys using the ELSGF method.

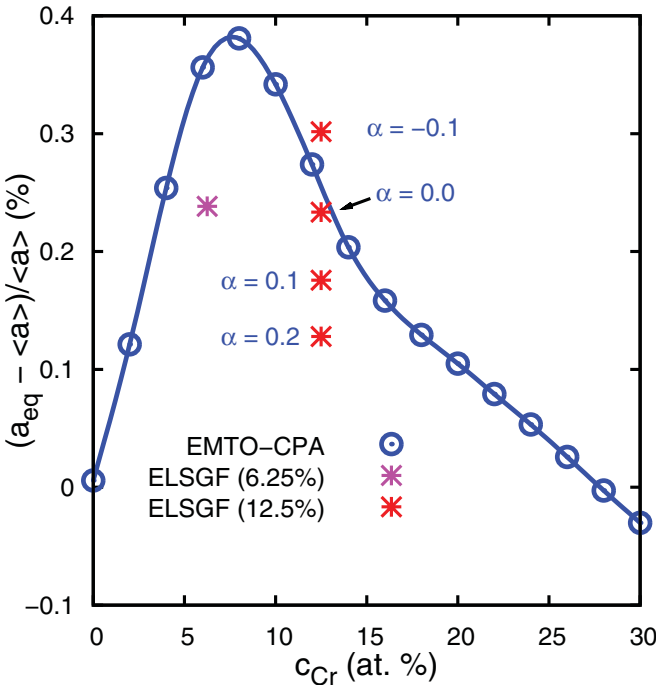

FIG. 7. (Color online) The dependence of the lattice constant on Cr concentration c_{Cr} and short-range-order parameter on the first coordination shell α_1 from the EMTO-CPA (circles) and ELSGF (stars) calculations (the solid line is a guide to the eye). Deviation of the lattice constant from Vegard's law is plotted. The only value obtained with ELSGF for $c_{Cr} = 6.25\%$ is evaluated for a completely disordered alloy ($\alpha_i = 0.0$ up to the eighth coordination shell).

In Fig. 7, we show the generalized-gradient-approximation[37] (GGA) results obtained by the usual EMTO-CPA method and by the ELSGF for the dependence of the equilibrium theoretical lattice constant on Cr concentration and the (Warren-Cowley) SRO parameter at the first coordination shell

$$\alpha_1 = \frac{\xi_1^{(2)} - \sigma^2}{1 - \sigma^2}. \tag{30}$$

The lattice constant is shown in relative units of the deviation from the average values (given by Vegard's law) for a given concentration.[38] The EMTO-CPA results are similar to those obtained in Ref. 34 and the ELSGF results have been obtained using a 256-atom supercell [8×4×4(×2) based on the cubic unit cell of the bcc lattice] for two alloy compositions of $Fe_{0.9375}Cr_{0.0625}$ and $Fe_{0.875}Cr_{0.125}$. In the first case, calculations have been done only for a completely random alloy without the SRO, while in the latter case, we have calculated the equilibrium lattice spacing of four supercells with $\alpha_1 = -0.1$, 0, 0.1, and 0.2. All these supercells are, of course, not ideally random, but the deviation of the other correlation functions from those in a random alloy has been small.[39]

As one can see, the ELSGF results for the random alloy are below the corresponding CPA results, hence closer to the experimental values.[34] One of the reasons is that the EMTO-CPA self-consistent calculations have been performed for fixed values of screening constants entering the definition of the onsite screened Coulomb interactions in the single-site DFT formalism.[20,21] Although they were determined for every

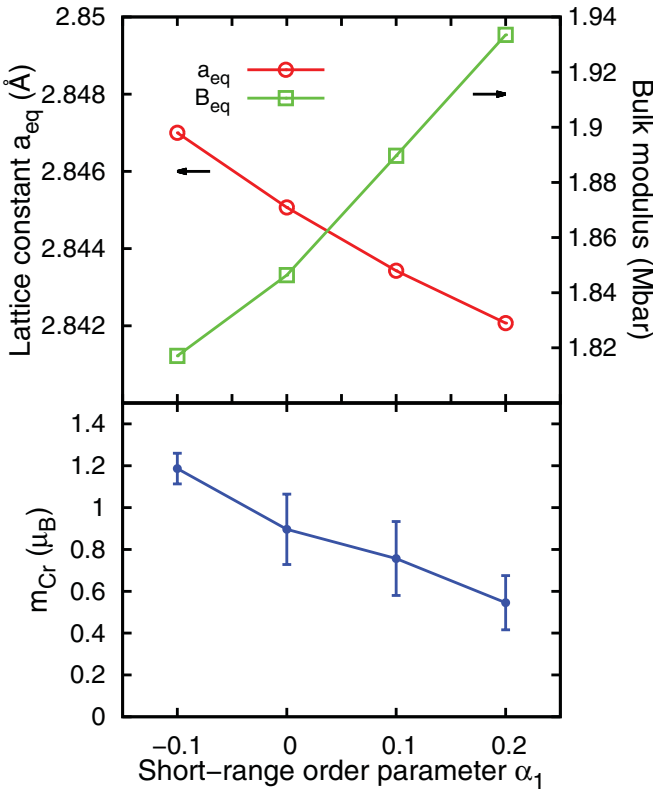

FIG. 8. (Color online) The dependence of the lattice constant (circles), bulk modulus (boxes), and magnetic moment of Cr (dots with whiskers) on the short-range-order parameter on the first coordination shell α_1. The whiskers in the bottom panel show the mean square root of the distribution of the magnitude of magnetic moments on Cr atoms.

composition,[34] they were kept constant in the total-energy calculations for different lattice constants. Local environment effects can also play an important role in this alloy since they affect the magnitude of the magnetic moment of Cr atoms dramatically.[32–34] A clear manifestation of this effect is the dependence of the equilibrium lattice constant in $Fe_{0.875}Cr_{0.125}$ on the SRO parameter: it decreases proportionally to the value of α_1 (see also the top panel of Fig. 8).

Let us note that the result is counterintuitive for negative values of the SRO parameter mean ordering tendency, i.e., preferential occupation of the corresponding coordination shell by the atoms of the opposite type, while positive values correspond to phase separation. The reason for such a reversal is the behavior of the local magnetic moments of Cr atoms. Their magnitude in Fe-rich Fe-Cr alloys is roughly proportional to the number of Fe nearest neighbors, and they, thus, go down with increasing the SRO parameter at the first coordination shell, as one can see at the bottom panel of Fig. 8. Decreasing magnetic moments of Cr result in the reduction of magnetic pressure, producing the effect of contraction. This example shows that SRO effects are especially important in magnetic alloys.

C. Elastic constants of $Fe_{0.875}Cr_{0.125}$

The full-charge-density formalism implemented in the EMTO method allows one to perform relatively accurate calculations of elastic properties of solids.[26] Although theoretical results are usually in a quite good agreement with available experimental data, the accuracy of such calculations, in particular related to the use of the single-site CPA in the DFT self-consistency, is not known.

When no alloys on sublattices are present, the ELSGF and EMTO methods are equivalent. In other words, the calculations of ordered systems are equivalent in accuracy, and this makes possible the direct comparison of the results on elastic properties obtained by the EMTO-CPA and ELSGF methods. To this end, we have again chosen Fe-Cr alloys, the elastic constants of which have been recently calculated by the EMTO-CPA method. In particular, we have calculated shear elastic moduli c' and c_{44} of the $Fe_{0.875}Cr_{0.125}$ alloy at the experimental lattice constant, 2.869 Å, in both the ferromagnetic and paramagnetic, i.e., DLM, states.

The ELSGF calculations have been done for a completely random alloy and with some amount of atomic SRO at the first coordination shell $\alpha_1 = 0.1$. The alloys have been modeled by 512-atom supercells ($8 \times 8 \times 8$ based on the primitive unit cell of the bcc lattice). The usual EMTO-CPA calculations have been done exactly for the same set up of k points ($39 \times 39 \times 39$ division of the full Brillouin zone in the Monkhorst-Pack method[40]), $l_{\max}$ cutoff (=3 for the partial waves inside atomic spheres), and other parameters.

For random alloys, an important difference between the EMTO-CPA and ELSGF calculations is that the DFT-based calculations of random alloys within single-site CPA should take into consideration the shift of the one-electron potential due to the onsite screened Coulomb interactions V_i^{scr}.[20,21] As has been demonstrated in Refs. 20 and 21,

$$V_i^{scr} = -\alpha_{scr}\frac{e^2 q_i}{S_{ws}}, \tag{31}$$

where q_i is the net charge in the atomic sphere of the ith alloy component, S_{ws} Wigner-Seitz radius, and α_{scr} the screening constant, which can be determined from the average values of the net charges and electrostatic potentials of the alloy components in supercell calculations.[20,21] The total energy in this case should be also corrected by the energy of the onsite screened Coulomb interactions E_{scr}, which in the case of a binary alloy is

$$E_{scr} = -\frac{e^2}{2}\sum_i c_i \alpha_{scr}\beta\frac{q_i^2}{S_{ws}}. \tag{32}$$

Here, c_i is the concentration of the ith alloy component, and an additional coefficient β takes care of the nonspherical contributions to the electrostatic energy ($\beta = 1$ if the multipole moment contributions to the electrostatic energy and potential are neglected).[21]

To do accurate single-site DFT-CPA calculations of the total energy of a random alloy, one should first determine both screening constants α_{scr} and β. This can only be done in supercell calculations, which enables one to go beyond the single-site approximation and determine the electrostatic energy and potential accurately. Obviously, such calculations

TABLE I. Elastic constants (in Mbar) of the $Fe_{0.875}Cr_{0.125}$ random alloy with and without SRO at the first coordination shell obtained by the EMTO-CPA, ELSGF, and PAW methods in the ferromagnetic and DLM states.

	ELSGF		EMTO CPA	PAW
Constant	$\alpha_1 = 0$	$\alpha_1 = 0.1$	($\alpha_1 = 0$)	($\alpha_1 = 0$)
c_{44}-FM	1.063	1.090	1.099	0.900
c_{44}-DLM	1.196	1.149	1.194	
c'-FM	0.705	0.741	0.740	0.555
c'-DLM	0.217	0.226	0.231	

are computationally very demanding, and the screening constants are, therefore, usually assumed to be constant for a given alloy, or at most have some concentration dependence.[34] In our EMTO-CPA calculations here, we determine screening constants from the corresponding ELSGF calculations for the initial undistorted bcc structure. In the FM calculations, we get $\alpha_{scr} = 0.7129$ and in the DLM calculations, $\alpha_{scr} = 0.778$.

The ELSGF calculations have been done with LIZ = 3 for the undistorted bcc lattice (two nearest-neighbor coordination shells for every site) and LIZ = 5 for the distorted lattices. The shear moduli have been determined from fitting the total energies of the alloy for five distortions with the step 1 and 0.5% in the cases of c' and c_{44}, respectively. The results of the calculations are presented in Table I.

As one can see from the table, the EMTO-CPA calculations overestimate (in this particular case, of course) both elastic constants. In the case of ferromagnetic calculations, this results from the assumption of the independence of the screening constants α_{scr} on the amount of deformation. In Fig. 9, we demonstrate that the assumption is not really accurate. The screening constants have been determined in the corresponding

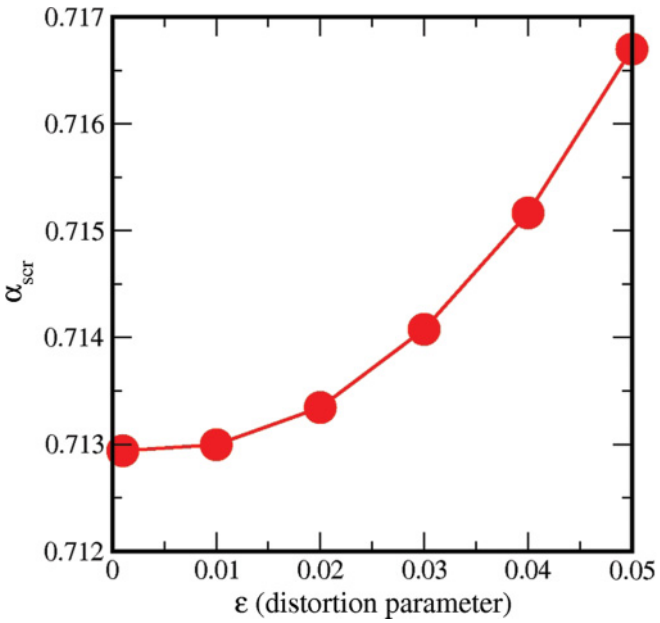

FIG. 9. (Color online) The screening parameter α_{scr} as a function of the distortion parameter in the calculation of c' in the ferromagnetic $Fe_{0.875}Cr_{0.125}$ random alloy.

ELSGF calculations as

$$\alpha_{scr} = -e^2 S_{ws} \frac{\langle V_i \rangle - \bar{V}}{\langle q_i \rangle}, \tag{33}$$

where $\langle V_i \rangle$ and $\langle q_i \rangle$ are the average values of the electrostatic potential and net charge of the atomic sphere of the ith alloy component in the supercell, and $\bar{V} = \sum_i c_i \langle V_i \rangle$ ($\bar{V} = 0$ in the absence of the multipole-moment contributions). The screening constant does not depend on the alloy component in the case of binary alloys, but it becomes component dependent if the number of alloy components is greater than two.

The screening constant growing with the deformation parameter implies the decrease of the screened Coulomb-interaction energy and, as a result, of the total energy of the alloy. This produces the effect of softening of the elastic constants. In CPA calculations, this effect is neglected and higher values of the shear moduli are obtained. It is interesting to note that the phase-separation type of the atomic SRO leads to the increase of both shear moduli by about the same 5% as the error coming from the incorrect electrostatics in the EMTO-CPA calculations.

There is also a noticeable effect of the magnetic state on elastic properties. Going over from FM to the DLM state in $Fe_{0.875}Cr_{0.125}$ results in a significant drop of c' by about a factor of 3, and the c_{44} constant increases by about 10% (more thoroughly, this system is discussed in Ref. 41). It is clear that the effect of the atomic SRO on the elastic constants in FeCr alloys in the paramagnetic state is much less pronounced than in the ferromagnetic case. The difference between EMTO-CPA and ELSGF calculations is also small in the paramagnetic state. This weak sensitivity of the strain with respect to the magnetic moment, as well as the screening constant, is due to isotropy of the system in this case.

In Table I, we also show the results of the projector-augmented-wave[42,43] (PAW) calculations of the random $Fe_{0.875}Cr_{0.125}$ alloy that has been modeled by a 128-atom supercell.[41] Clearly, the present implementation of the total-energy full-charge-density technique produces quite a substantial error, of about 25%–30%, and this issue needs a separate investigation. Nevertheless, ELSGF seems to be a versatile and sufficiently accurate tool to investigate complex effects of the atomic SRO, especially when it comes to the impact of a magnetic state on various properties of alloys.

D. Surface-segregation energies of Cr on Fe(001) and Fe(011)

Apart from direct applications of LSGF to random alloys, the method can also be used to study inhomogeneous systems, such as surfaces, interfaces, impurities, etc. One of such prospective applications is the calculation of solution and segregation energies in cases when the size mismatch of alloying components is small (and the relaxation energy is small). The advantage of the LSGF formalism here is that the LIZ effectively cuts off a spurious interaction between alloying species. This property is very important for systems either with strong and long-range effective interactions and/or exhibiting strong concentration dependence of the alloying behavior. This is exactly the case of Fe-Cr alloys, where (as has been demonstrated in Ref. 44) the size of the supercell plays a very

important role in the determination of the surface-segregation energy.

An alternative way to calculate this energy is to use the CPA-based method.[22] However, in the presence of a substantial charge transfer between atomic spheres of the alloy components, it is very difficult to accurately take care of the onsite screened Coulomb interactions for surface alloys, and this can lead to a large error as was demonstrated in Ref. 45.

In this section, we apply the ELSGF method to the calculation of the surface-segregation energy of Cr onto the (001) and (110) surfaces of bcc Fe. Although this energy has nothing to do with the corrosion resistance of steels, as has been frequently claimed, it is anyway an important thermodynamic quantity.

There exist several calculations of the surface-segregation energies for this system,[44,46–49] but all of them have been done for the ferromagnetic state. An additional advantageous feature of LSGF is that the surface-segregation energy (or more general surface-related quantities) can be obtained in the paramagnetic (DLM) state, which is important because phase transformations usually take place in this state.

The surface-segregation energy is the energy difference between two configurations of an impurity atom: one with the impurity being in the surface layer and another one when it is in the bulk. The supercell approach is then reduced to the calculations of such two systems. The surface in this case can be modeled using a slab geometry with a vacuum region, which, in the case of the EMTO method, is filled with empty spheres. In our case, we have chosen a 20-layer slab for the (001) surface (13 atomic and 7 vacuum layers) and a 14-layer slab (9 atomic and 5 vacuum layers) for the (110) surface. The corresponding 20- and 14-atom unit cells have been used to define the effective medium, while the entire supercells have been constructed from the initial slab unit cells by translations in the plane parallel to the surface layer repeating the unit cells 6×6 and 8×6 times for the (100) and (110) surfaces, respectively. The supercell has consisted, thus, of 672 sites for the (110) surface and of 720 sites for the (001) surface.

In the ELSGF calculations, the LIZ has consisted of a central atom and its two nearest-neighbor (bcc) coordination shells (LIZ = 3). The self-consistent calculations have been done for the room-temperature experimental lattice constant of Fe, 2.86 Å, using local density approximation (LDA).[50–54]

The results of the calculations are presented in Table II. They can be compared to the results for the (100) surface obtained by Ponomareva *et al.*,[44] who also did calculations for the room-temperature lattice constant of Fe using the PAW method and found that the surface-segregation energy of Cr on the (100) surface of Fe is 0.190 eV. Our ELSGF result, 0.204 eV, is in a good agreement with the PAW result.

TABLE II. Surface-segregation energies (in eV) of Cr on the (100) and (110) surfaces of Fe in the FM and DLM states.

	Fe(110)	Fe(100)
FM	0.068	0.204
DLM	0.144	0.190

The segregation energies obtained in Ref. 49 are significantly lower than those in Table II: −0.001 and 0.076 eV for the (110) and (100) surfaces, respectively, most probably because they were obtained for a relatively small supercell and for the theoretical equilibrium lattice constant of Fe. As was demonstrated by Ponomareva *et al.*,[44] both these parameters strongly affect the results, and we therefore believe that our results are quantitatively accurate.

Finally, one can see that there is quite a pronounced effect of the magnetic state on the segregation energy of the (110) surface: the surface-segregation energy in the DLM (paramagnetic) state is almost doubled compared to that in the FM state. This means that at elevated temperatures, relevant to experimentally achievable equilibrium, the surface segregation of Cr atoms toward the (110) should be reduced. Let us note that this surface has an important role in the thermodynamics since it is the most closely packed surface in the case of the bcc structure, and thus has the lowest energy. It is also clear that such a result is extremely difficult, if possible, to obtain at the same level of accuracy by any other existing method.

IV. CONCLUSION

We have demonstrated that the ELSGF method can be a rather accurate and versatile tool for studying local environment effects in random alloys as well as in inhomogeneous systems, such as surfaces and interfaces. In particular, we have applied it to the Fe-rich FeCr alloy and found that an intimate coupling between SRO and the equilibrium lattice constant as well as elastic properties results from the strong sensitivity of Cr magnetic moments on the local environment. Among the advantages of the method is its order-N scaling, which makes the implementation easy to parallelize and enables one to treat large supercells consisting of $N \sim 10^4$–10^5 atoms. In addition, the capability to treat the high-temperature paramagnetic state renders possible investigating phase transitions in magnetic alloys.

Compared to the KKR-ASA implementation, ELSGF has a much more accurate normalization of states and can, therefore, be applied to systems with a distorted structure and large ion-size mismatches. This feature opens up a completely new possibility to take into account random relaxations in alloys within ELSGF. Formally, this amounts to introducing an additional perturbation of the structure constants into the Dyson equation (18). Accurate evaluation of the kinetic energy is a necessary prerequisite for such an expansion in the structure-constant perturbation to give good results, which can be achieved by a full-charge-density self-consistent implementation of ELSGF.

Other implementations of LSGF are possible. For instance, a fully relativistic EMTO-LSGF method can be realized by replacing Green's functions in spin-up and -down channels with full Dirac 2×2-spinor Green's functions. A full-potential KKR implementation is also straightforward.

ACKNOWLEDGMENTS

The authors would like to thank I. A. Abrikosov and L. Vitos for discussions. O.E.P. expresses gratitude to A. Lichtenstein for useful comments. A.V.R. and B.J.

acknowledge the financial support of the support of the Swedish Research Council (VR) and European Research Council (ERC). Computer resources for this study have been provided by the Swedish National Infrastructure for Computing (SNIC) and MATTER Network, at the National Supercomputer Center (NSC), Linköping. This work was partly performed within the VINNEX center Hero-m, financed by the Swedish Governmental Agency for Innovation Systems (VINNOVA), Swedish industry, and the Royal Institute of Technology (KTH).

[1] P. Soven, Phys. Rev. **156**, 809 (1967).
[2] D. W. Taylor, Phys. Rev. **156**, 1017 (1967).
[3] J. Korringa, Physica (Amsterdam) **13**, 392 (1947).
[4] W. Kohn and N. Rostoker, Phys. Rev. **94**, 1111 (1954).
[5] B. L. Gyorffy, Phys. Rev. B **5**, 2382 (1972).
[6] I. Abrikosov, Y. Vekilov, and A. Ruban, Phys. Lett. A **154**, 407 (1991).
[7] J. Kudrnovský, P. Weinberger, and V. Drchal, Phys. Rev. B **44**, 6410 (1991).
[8] L. Vitos, I. A. Abrikosov, and B. Johansson, Phys. Rev. Lett. **87**, 156401 (2001).
[9] A. Mookerjee, J. Phys. C: Solid State Phys. **6**, L205 (1973); **6**, 1340 (1973).
[10] M. Tsukada, J. Phys. Soc. Jpn. **26**, 684 (1969).
[11] R. Mills and P. Ratanavararaksa, Phys. Rev. B **18**, 5291 (1978).
[12] D. A. Rowlands, J. B. Staunton, and B. L. Györffy, Phys. Rev. B **67**, 115109 (2003).
[13] D. A. Biava, S. Ghosh, D. D. Johnson, W. A. Shelton, and A. V. Smirnov, Phys. Rev. B **72**, 113105 (2005).
[14] D. A. Rowlands, X.-G. Zhang, and A. Gonis, Phys. Rev. B **78**, 115119 (2008).
[15] Let us note that this is not the case for nonmetallic systems, where the effective short-range screening is absent. Such systems require the use of special techniques[51–54] and very large supercells exactly for the reason that all types of interactions are extremely long range and strong. At the same time, the methods based on the CPA do not work in this case since the CPA can not provide accurate description of the state in the band gap and close to the band edge, which are the most important from the point of view of the majority of the physical properties.
[16] I. A. Abrikosov, A. M. N. Niklasson, S. I. Simak, B. Johansson, A. V. Ruban, and H. L. Skriver, Phys. Rev. Lett. **76**, 4203 (1996).
[17] I. A. Abrikosov, S. I. Simak, B. Johansson, A. V. Ruban, and H. L. Skriver, Phys. Rev. B **56**, 9319 (1997).
[18] A. Gonis and J. W. Garland, Phys. Rev. B **16**, 2424 (1977).
[19] Y. Wang, G. M. Stocks, W. A. Shelton, D. M. C. Nicholson, Z. Szotek, and W. M. Temmerman, Phys. Rev. Lett. **75**, 2867 (1995).
[20] A. V. Ruban and H. L. Skriver, Phys. Rev. B **66**, 024201 (2002).
[21] A. V. Ruban, S. I. Simak, P. A. Korzhavyi, and H. L. Skriver, Phys. Rev. B **66**, 024202 (2002).
[22] A. Ruban and H. Skriver, Comput. Mater. Sci. **15**, 119 (1999).
[23] O. Andersen, O. Jepsen, and G. Krier, in *Lectures on Methods of Electronic Structure Calculations*, edited by V. Kumar, O. Andersen, and A. Mookerjee (World Scientific, Singapore, 1994), p. 63.
[24] L. Vitos, H. Skriver, B. Johansson, and J. Kollr, Comput. Mater. Sci. **18**, 24 (2000).
[25] L. Vitos, Phys. Rev. B **64**, 014107 (2001).
[26] L. Vitos, *Computational Quantum Mechanics for Materials Engineers* (Springer-Verlag, London, 2007).
[27] E. Kabliman, P. Blaha, K. Schwarz, O. E. Peil, A. V. Ruban, and B. Johansson, Phys. Rev. B **84**, 184206 (2011).
[28] B. L. Gyorffy, A. J. Pindor, J. Staunton, G. M. Stocks, and H. Winter, J. Phys. F: Met. Phys. **15**, 1337 (1985).
[29] One should note, however, that strictly speaking, the exact evaluation of the electrostatic potential and energy implies knowing the exact electron density of the entire supercell, and the latter is known only approximately in the LSGF calculations due to the use of the finite LIZ. For instance, in the case of the B2-NiAl alloy and LIZ $= 1$, the multipole-moment contributions for a specific coordination of Ni and Al atoms are replaced by those for the effective medium beyond the first coordination shell (see Ref. 21). This means that care should be taken to provide a desired atomic-distribution correlation function in the supercell to avoid a spurious electrostatic contribution. That being said, the effective electrostatic interactions in disordered metals are well screened within the first several coordination shells (Refs. 20 and 21), which substantially alleviates the problem for a sufficiently large supercell containing about 500 atoms or more.
[30] P. Olsson, I. Abrikosov, L. Vitos, and J. Wallenius, J. Nucl. Mater. **321**, 84 (2003).
[31] P. Olsson, I. A. Abrikosov, and J. Wallenius, Phys. Rev. B **73**, 104416 (2006).
[32] T. P. C. Klaver, R. Drautz, and M. W. Finnis, Phys. Rev. B **74**, 094435 (2006).
[33] A. V. Ruban, P. A. Korzhavyi, and B. Johansson, Phys. Rev. B **77**, 094436 (2008).
[34] P. A. Korzhavyi, A. V. Ruban, J. Odqvist, J.-O. Nilsson, and B. Johansson, Phys. Rev. B **79**, 054202 (2009).
[35] M. Hennion, J. Phys. F: Met. Phys. **13**, 2351 (1983).
[36] I. Mirebeau, M. Hennion, and G. Parette, Phys. Rev. Lett. **53**, 687 (1984).
[37] J. P. Perdew, K. Burke, and M. Ernzerhof, Phys. Rev. Lett. **77**, 3865 (1996).
[38] There is a quite strong deviation of the zero-temperature theoretical results from the room-temperature experimental data for the concentration dependence of the equilibrium lattice constants in Fe-Cr alloy (see, for instance, Ref. 34). Here, we avoid any discussion of a possible reason since it is beyond the subject and the aim of this paper. This problem will be addressed elsewhere.
[39] Specifically, for $Fe_{0.9375}Cr_{0.0625}$, the pair SRO parameters have been fixed to 0.0 up to the eighth coordination shell; in the case of $Fe_{0.875}Cr_{0.125}$ for $\alpha_1 = 0.0$, the first small nonzero value has appeared at the seventh coordination shell ($\alpha_7 \approx 0.011$), and for $\alpha_1 \neq 0.0$, the values at the other coordination shells have been kept within 30% of α_1.
[40] H. J. Monkhorst and J. D. Pack, Phys. Rev. B **13**, 5188 (1976).
[41] V. I. Razumovskiy, A. V. Ruban, and P. A. Korzhavyi, Phys. Rev. Lett. **107**, 205504 (2011).
[42] P. E. Blöchl, Phys. Rev. B **50**, 17953 (1994).

[43]G. Kresse and D. Joubert, Phys. Rev. B **59**, 1758 (1999).
[44]A. V. Ponomareva, E. I. Isaev, N. V. Skorodumova, Y. K. Vekilov, and I. A. Abrikosov, Phys. Rev. B **75**, 245406 (2007).
[45]A. U. Nilekar, A. V. Ruban, and M. Mavrikakis, Surf. Sci. **603**, 91 (2009).
[46]B. Nonas, K. Wildberger, R. Zeller, and P. H. Dederichs, Phys. Rev. Lett. **80**, 4574 (1998).
[47]A. V. Ruban, H. L. Skriver, and J. K. Nørskov, Phys. Rev. B **59**, 15990 (1999).
[48]W. T. Geng, Phys. Rev. B **68**, 233402 (2003).
[49]A. Kiejna and E. Wachowicz, Phys. Rev. B **78**, 113403 (2008).
[50]J. P. Perdew and Y. Wang, Phys. Rev. B **45**, 13244 (1992).
[51]T. G. Dargam, R. B. Capaz, and B. Koiller, Phys. Rev. B **56**, 9625 (1997).
[52]L.-W. Wang, L. Bellaiche, S.-H. Wei, and A. Zunger, Phys. Rev. Lett. **80**, 4725 (1998).
[53]T. B. Boykin, N. Kharche, G. Klimeck, and M. Korkusinski, J. Phys.: Condens. Matter **19**, 036203 (2007).
[54]V. Popescu and A. Zunger, Phys. Rev. Lett. **104**, 236403 (2010).